Visible-Light Driven Photocatalytic Coupling of Benzylamine Over Titanium-Based MIL-125-NH_2 Metal-Organic Framework: a Mechanistic Study

Jenny G. Vitillo,[a] Davide Presti,[b] Ignacio Luz,[c,†] Francesc X. Llabrés i Xamena,[c] Silvia Bordiga[d]*

[a]Department of Science and High Technology and INSTM, University of Insubria, Via Valleggio 9, 22100 Como, Italy.

[b]CINECA Supercomputing Centre, Department of SuperComputing Applications and Innovation, HPC-SCAI, 40033 Casalecchio di Reno, Italy.

[c]Instituto de Tecnología Química, Universitat Politècnica de València, Consejo Superior de Investigaciones Científicas, Avda. de los Naranjos, s/n, 46022 Valencia, Spain.

[d]Department of Chemistry, NIS Center and INSTM, University of Turin, via Gioacchino Quarello 15A, I-10135 Torino, Italy.

KEYWORDS. Metal-organic framework; MIL-125-NH_2; amine oxidative coupling; photocatalysis; *N*-benzylidenebenzylamine; titanium.

ABSTRACT. Imines are important building blocks in organic chemistry. Titanium-based metal-organic framework MIL-125-NH_2(Ti) can photocatalyze, under visible light and at room temperature, the selective aerobic oxidation of benzylamine to *N*-benzylidenebenzylamine. We investigated the reaction mechanism using catalytic tests, *ex situ* infrared spectroscopy, and density functional calculations. In the dark, the presence of MIL-125-NH_2(Ti) alone does not improve the reaction yield with respect to a blank experiment. This poor catalytic performance in the dark is associated to the absence of polarizing species on the MOF surface, as confirmed by acetonitrile adsorption. Excitation with different spectral regions evidenced the determinant role of the $450 < \lambda < 385$ nm range for the catalyst photoactivation. The calculations show that the last step of the reaction would have an energy barrier of 206 kJ mol^{-1} in anhydrous conditions, while it decreases to 91 kJ mol^{-1} only if the mechanism is mediated by two water molecules.

1. INTRODUCTION

Imines are among the most important intermediates in the synthesis of organic compounds in general[1] and of pharmaceuticals in particular.[2] These compounds are traditionally synthesized through the dehydrated condensation of the corresponding amine with an aldehyde or a ketone,[2] reactions characterized by a low selectivity due to the reactive nature of the carbonyl group.[3] Direct oxidation of amines overcome this problem, although the oxidants used (e.g. *N*-tert-butylphenylsulfinimidoyl chloride) are costly and not environment friendly.[4] The use dioxygen as oxidant in the reaction would make the direct oxidation of amines the route of choice for the synthesis of these important compounds.[5] Nevertheless, it is often accompanied by the formation

of several by-products.[1] The discovery of new selective catalysts for this reaction is then a hot topic of research.[6-13]

Metal organic frameworks (MOFs) are materials that have shown exceptional performances in several fields.[14] Their structure is constituted by metal/metal oxide clusters connected through organic molecules. It is possible to modify separately the inorganic and the organic building units to tailor the material for a specific use. MOFs have been already reported as efficient catalyst and photocatalysts for several reactions,[15-20] and in particular for imine synthesis.[10, 21-22]. Photocatalytic oxidation of amines to imines is particularly appealing because it requires reaction temperature close to room temperature. Moreover, it has been recently proposed to be combined with water splitting for hydrogen production as a way to increase the valuable products of the reaction.[10, 23] Titanium-based MOFs have been reported as photocatalysts for many reactions,[24-27] due to their high thermal and chemical stability. MIL-125 family[28] is the most studied among them.[22, 25-26, 29-33] An important feature that makes interesting MIL-125(Ti) family for applications is their good stability upon water adsorption/desorption.[30] Their structure is constituted by $Ti_8O_8(OH)_4$ rings (see Figure 1a) interconnected by bitopic organic linkers, to form a centered cubic structure. The pores have a square bipyramid shape of dimensions 18 and 15 Å. The top of both pyramids is truncated and there a $Ti_8O_8(OH)_4$ ring is placed. The access to the cavity of guest molecules is guaranteed by the faces of the pyramids, being equilateral triangles with base of 11 Å.

Among MIL-125 analogous, MIL-125-NH_2(Ti) is the most studied one.[24-26, 28, 34] The presence of the –NH_2 group on the terephthalate linker of MIL-125-NH_2(Ti) changes not only the hydrophilicity and basicity of the MOF but also improves its photocatalytic properties.[35-36] In fact, MIL-125 is active as photocatalyst only under UV irradiation, whereas the additional NH_2 group expands its activity into the visible light range.[28] Moreover, as recently demonstrated by Santaclara

et al.,[35-36] the difference in photoexcitation of the two isomorphous materials is not limited to a different absorption profile. In fact, exactly as in MIL-125, the photoexcitation in MIL-125-NH_2 is a ligand-to-cluster charge transfer (LCCT)[37] where an electron is promoted from the linker to the $Ti_8O_8(OH)_4$ cluster reducing Ti^{4+} to Ti^{3+}. Unlike MIL-125(Ti), the presence of an electron donating substituent on the organic linker allows to increase the lifetime of the photogenerated hole by stabilising it on the amino group, intrinsically increasing its efficiency as photocatalyst.[35-36]

The photocatalytic activity of MIL-125-NH_2(Ti) for the aerobic oxidation of benzylamine to *N*-benzylidenebenzylamine was recently reported by Sun et al.[11-12] They have considered different reaction media, determining acetonitrile as the optimum solvent allowing to reach a conversion of 73% with a selectivity of 86% after 12 h of irradiation with a 300 W Xe lamp. The MOF structure was stable under the photocatalytic conditions used and the catalytic activity was verified to be stable upon cycling.[11-12] Several possible mechanisms can regulate the reaction.[3, 38] Sun et al.[11] suggested that the oxidation of benzylamine in MIL-125-NH_2(Ti) could pass through the oxidation of one benzylamine molecule to benzaldehyde (step a in Scheme 1). This is the step where the MOF will play its photocatalytic activity by converting O_2 to an O_2^- radical anion. An electron is transferred from a photogenerated Ti^{3+} center to O_2 with the formation of Ti^{4+} and O_2^-. Then, the benzaldehyde molecule undergoes a nucleophilic attack by a second benzylamine molecule (step (b)). The way the reaction proceeds to the formation of the imine can be very influenced by several factors as the pH and the reaction medium.[3, 38] We suggest steps (c) and (d) as in Scheme 1 as the most plausible ones in the experimental conditions used (aprotic solvents, basic conditions).[3, 38] The zwitterionic species formed in step (b) undergoes in step (c) a first intramolecular proton transfer with the formation of the carbinolamine. Step (c) can proceed only through the mediation

of water molecules:[38] in fact, the high strain four-ring reported in Scheme 1 is characterized by a high formation energy. This is significantly lowered in presence of water molecules being the four ring replaced by a six- or eight-ring with a significant decrease in the activation energy.[38] The last step of the reaction, step (d), corresponds to the intramolecular proton transfer in the carbinolamine species (**CA** in the following) with the formation of imine and elimination of one water molecule (**BI** intermediate) through the transition state **TS** (last row in Scheme 1). As step (c), also step (d) requires the formation of a high strain four-ring in the transition state. Nevertheless, unlike step (c), in this case the presence of water molecules in similar reactions[38] is less beneficial, as they cannot completely remove the strain of the ring, because of the presence of the (O=C)-NH bond. Step (d) is then the rate determining step in imine formation reactions for pH≥7.[3, 38] Few theoretical studies have been reported in literature on imine formation mechanisms[3, 38-39] and none on the *N*-benzylidenebenzylamine one.

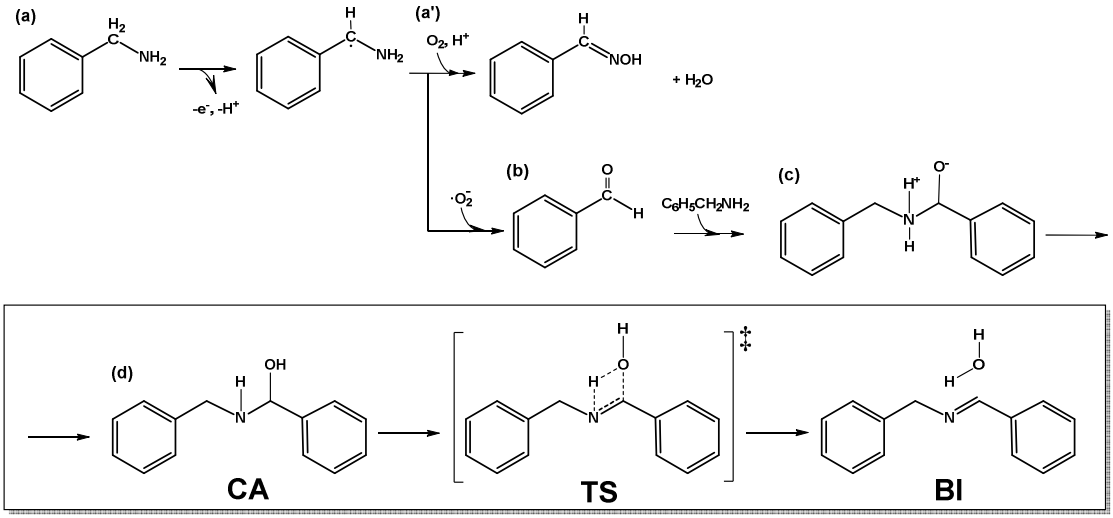

Scheme 1. Mechanism proposed for the aerobic benzylamine coupling reaction to *N*-benzylidenebenzylamine photocatalyzed by MIL-125-NH_2(Ti). MIL-125-NH_2(Ti) would play a

role as photocatalyst in step (a) and (a'). The rectangle highlights the reaction step investigated using DFT methods in this work.

In the present study, we have synthesized a MIL-125-NH_2(Ti) sample using a recipe slightly modified with respect to those reported in the literature. We have assessed the quality of the material through comparison of its experimental Powder X-Ray Diffraction (XRD) pattern, infrared spectrum, and surface area with the corresponding theoretical values obtained for a periodic model optimized using Kohn-Sham Density Functional Theory (KS-DFT) methods. MIL-125-NH_2 activity as photocatalyst for benzylamine oxidation in acetonitrile was tested irradiating the batch with a Xe lamp for 6 h by selecting different irradiating conditions. *Ex situ* infrared spectroscopy characterization of the reaction was also conducted in order to identify possible reaction intermediates. Cluster calculations have been performed on step (d) in Scheme 1 to determine the feasibility of the proposed mechanism in our experimental conditions. In particular, we have evaluated the effect of the presence of water molecules on the energetics of the **CA** $\rightarrow$ **BI** conversion. These results have been exploited for the identification of strategies aimed at improving the efficiency of the reaction.

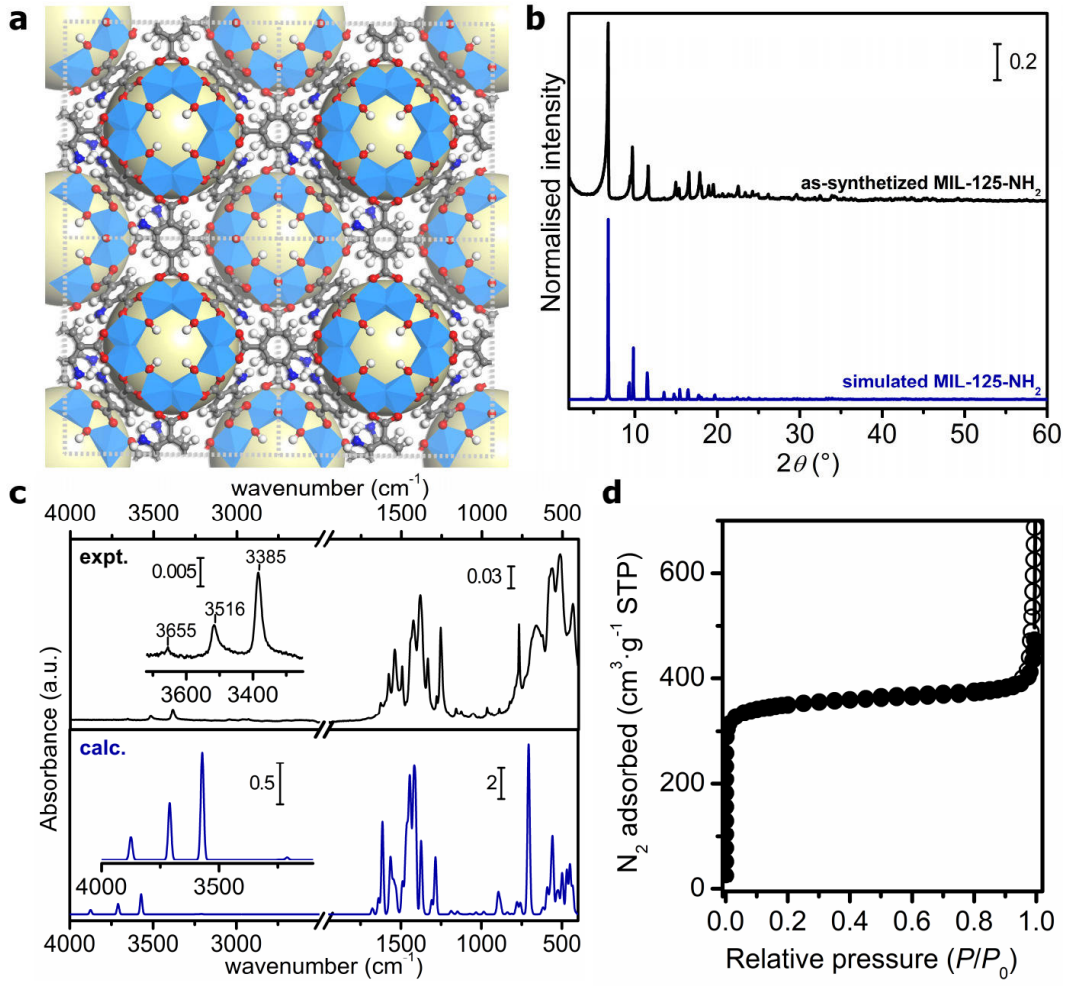

Figure 1. MIL-125-NH_2(Ti) structure and material characterization. **a.** MIL-125-NH_2 structure as obtained from optimization at the B3LYP-D*/6-31G level. View along the [010] direction. The C atoms are reported in gray, H atoms in white, O in red, Ti in light blue (octahedron), N in blue. The pore voids are represented as light yellow spheres, allowing appreciating their bcc arrangements. **b.** Powder X-ray diffraction pattern of MIL-125-NH_2: experimental (as-synthesized material, in air, black curve), theoretical pattern (blue curve). The theoretical pattern has been calculated using the B3LYP-D*/6-31G optimized structure. **c.** Infrared spectrum of a fully desolvated MIL-125-NH_2(Ti) (black curve) compared to the corresponding theoretical (blue line).

d. Excess nitrogen isotherms at 77 K (full scatters: adsorption branch; empty scatters: desorption branch).

2. MATERIALS AND METHODS

Detailed description of the theoretical methods used and of the synthesis and characterization of MIL-125-NH_2(Ti) is reported in the Supporting Information.

Photocatalytic tests. The reaction was performed by contacting benzylamine (0.1 mmol, 10.7 mg) and 1.5 mg of catalyst in 2 ml CH_3CN at room temperature. The solution, kept under stirring (600 rpm), was irradiated with a Hamamatsu 150W Xe lamp for 6 h, either without optical filters or with two different filters, for λ >385 nm and λ >450 nm, respectively. For comparison, the yields of the reaction at 60°C in the dark or in absence of the catalyst have been also obtained.

3. RESULTS AND DISCUSSION

3.1 Material characterization.

Characterization of the synthesized material and the comparison of the experimental data set so obtained with reference values from the periodic model confirmed the purity of the MIL-125-NH_2(Ti) sample and its negligible concentration of defects (see Table S1). The X-ray powder diffraction pattern measured for the synthesized material is reported as black line in Figure 1b, along with the corresponding theoretical pattern (blue line). In Table S1, it is also shown the very good agreement among the theoretical and the experimental cell parameters.

Adsorption measurements are a more sensitive tool than X-ray diffraction to detect the presence of defects and impurities in MOFs.[40] In particular, the presence of mesopores, that are often associated with structural defects or collapse in this class of materials, can be easily detected by recording adsorption isotherms of low interacting molecules at their condensation temperature. Excess nitrogen isotherms obtained at 77 K for MIL-125-NH_2 are reported in Figure 1d. These isotherms are of type I, typical of microporous materials, without mesopores.[41] The experimental Langmuir surface area is equivalent within the experimental error to the value calculated on the theoretical structure (1557 vs. 1801 $m^2\ g^{-1}$, see Table S1).

Infrared spectroscopy is another tool that can be used to assess the quality of MOF materials. Defects in carboxylate-based materials are often associated with the partial hydrolysis of the structure with the creation of hydroxo species that give extra peaks in the 3700-3500 cm^{-1} region and a large band associated to H-bond interaction in the 3600-2500 cm^{-1} range.[42] Meanwhile, the presence of impurities and extra phases (such as titanium (oxo)hydroxide species) can be detected by comparison with a reference spectrum. The ATR-FTIR spectrum of MIL-125-NH_2(Ti) is reported as black line in Figure 1c. In Figure 1c it is also reported the B3LYP-D*/6-31G computed infrared spectrum of MIL-125-NH_2(Ti) as a blue line. The similarities of the two spectra allow to rule out the presence of extra phases. In particular, in the –OH stretching region a single peak is present at 3655 cm^{-1}, indicating the presence of a single type of isolated hydroxo species, thus supporting at the atomic scale the low defectivity of the structure. The absence of a peak at 1690 cm^{-1} indicates the full removal of DMF in the washing procedure.[42] A full assignment of all the IR peaks with the help of the calculations is reported in Table S3.

Diffuse reflectance UV-Vis spectra of MIL-125-NH_2 is reported as light yellow curve in Figure 2b. The spectrum obtained for the linker is also reported as dark yellow curve. The MOF optical

features are similar to those reported previously[28, 36, 43] with two bands with maxima at 277 and 373 nm, associated with Ti-O oxo-cluster absorption and ligand to cluster charge transfer (LCCT) transitions, respectively. MIL-125-NH_2 absorption spectrum zeroes at 498 nm that is in the visible range. The experimental band gap (calculated as the lowest energy inflection point of the UV-Vis spectrum) is estimated to be 2.95 eV (420 nm), in good agreement with previous results and in excellent agreement with the calculations (2.96 eV, see Table S1).

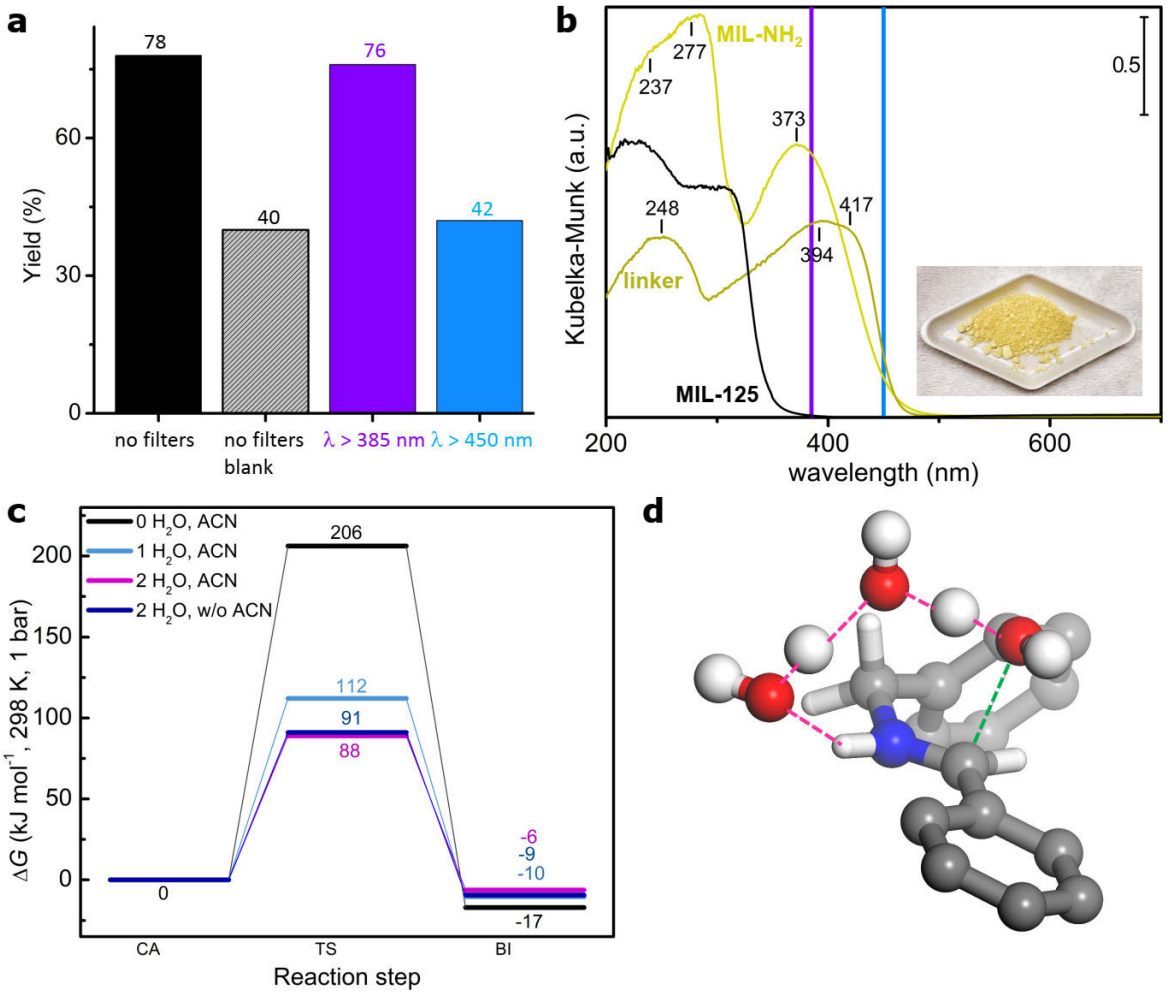

Figure 2. MIL-125-NH_2(Ti) as a catalyst for benzylamine coupling reaction. **a.** Reaction yield of *N*-benzylidenebenzylamine (BI) using different irradiation conditions at room temperature (see Table 1). The yield obtained without the catalyst is also reported for comparison (grey bar). **b.** Diffuse reflectance UV-Vis spectra of MIL-125(Ti) (black curve), MIL-125-NH_2(Ti) (light yellow curve), and 2-amino-terephtalic acid (dark yellow curve) as obtained in air in a 1:100 dilution in weight in Teflon. The wavelength positions of the > 385 and > 450 nm filters used in the catalytic tests are marked with a violet and a light blue vertical line, respectively. **c.** Reaction profile for the last step of the benzylamine coupling reaction to *N*-benzylidenebenzylamine in acetonitrile (step (d) in Scheme 1) as calculated at the M06/6-311++G(3df,2p) considering the reaction being mediated by 0 (black line), 1 (light blue line), and 2 water molecules (violet line). For the two water molecules case, the profile calculated in the absence of the solvent (dark blue line) is also reported for comparison. **d.** Transition state structure for the two water-mediated case in CH_3CN as optimized with M06/6-311G(3df,2p). Color code as in Figure 1. The hydrogen atoms of the phenyl rings are omitted for clarity.

3.1.1. Surface acidity. In a MOF without open metal site such as MIL-125-NH_2(Ti), the structural Ti-OH groups can have a role in determining the activity of the MOF as an acid catalyst. In order to measure the polarity of these groups, and then to determine if they can have a role in the reaction, we have used the perturbation of infrared signals of deuterated acetonitrile upon adsorption on the MOF surface. This adsorbate can also evidence the presence of other polarizing species, such as coordinatively unsaturated Ti^{4+} Lewis acid sites associated to defects. CD_3CN is in fact a suitable molecular probe for monitoring both surface acidity and basicity.[44-46] The spectra recorded on MIL-125-NH_2(Ti) are reported in Figure 3. They show two signals in the C-N

stretching region: a main peak at 2261 cm^{-1} and a shoulder at 2272 cm^{-1}. The peak at 2261 cm^{-1} corresponds to the molecules unperturbed (physisorbed) inside the MOF pores. The shoulder at 2272 cm^{-1} can be assigned to the formation of Ti-OH···$NCCD_3$ and –NH_2···$NCCD_3$ adducts. The interaction with Ti-OH groups is confirmed by the perturbation of OH bands upon CD_3CN dosing both in the 3700-3500 cm^{-1} (-OH stretching) and 980-920 cm^{-1} (-OH bending, see Figure S2). In particular, the band at 3655 cm^{-1} experiences a significant decrease in intensity with corresponding broadening. A significant perturbation of the amino bands is also observed (see Figure S2). The small blue shift of the ν(C≡N) band at 2272 cm^{-1} of adsorbed CD_3CN with respect to the 2261 cm^{-1} of physisorbed CD_3CN is of the same order to that observed for acetonitrile interacting with silanols in zeolites,[46] indicating a very low acidity of the Ti-OH species of MIL-125-NH_2. Moreover, the two signals growth in parallel, indicating that the adsorption energy of CD_3CN on the MOF surface species is comparable with its liquefaction energy. No bands are observed at >2300 cm^{-1},[46] allowing to rule out the presence of exposed Ti(IV) Lewis acid sites on the MOF surface. Also the position of the symmetric C-D stretching signal (2111 cm^{-1}) suggests a very low interaction energy, being coincident with its liquid-like value.[47] The acetonitrile molecules were fully removed from the MOF surface at beam temperature (40-60 °C) upon pumping. We can then say that there are not strong adsorption centers on the MOF surface. Moreover, being the interaction of acetonitrile with the MOF very weak, would suggest acetonitrile as an ideal dispersing medium in photocatalytic reactions involving MIL-125-NH_2(Ti).

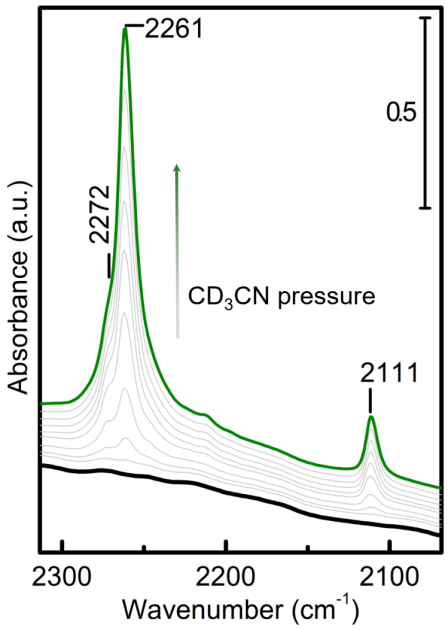

Figure 3. FTIR spectrum of MIL-125-NH_2(Ti) in contact with 1 mbar of CD_3CN (green line) at beam temperature. The other spectra were recorded by decreasing gradually CD_3CN equilibrium pressure to vacuum (light grey curves). The spectrum obtained after degassing one hour at beam temperature was coincident with the spectrum recorded initially in vacuum (black curve) and then it is not reported. a.u. = absorbance units.

3.2. Benzylamine oxidation reaction

3.2.1. Catalytic tests. The catalytic activity of MIL-125-NH_2(Ti) was tested in four different irradiation conditions in order to identify the spectral range that more influence the photoactivity of the MOF. Besides using the Xe lamp in its full spectral range, two different filters were adopted in order to select only the photons with either a wavelength $\lambda > 385$ nm or $\lambda > 450$ nm, respectively. These filters were chosen based on the UV-Vis spectrum of the MOF that shows a strong

absorption in the visible in the region, due to the presence of the amino functionality on the linker (see Figure 2b). Additionally, the reaction was carried out in the dark by heating the sample at 60 °C. This temperature was selected to account for the heating effect of the Xe lamp, occurring in the irradiated experiments. As the reaction medium, we used acetonitrile based on the work of Sun et al. [11] that indicates acetonitrile as the optimum medium in terms of conversion and selectivity. Finally, we have performed a parallel set of reactions in the absence of the MOF to verify its photocatalytic activity.

The results obtained from the catalytic tests are reported in Table 1 and in Figure 2a. In Table 1, it is reported a small review on the conversions obtained for other MOFs[10, 22, 48-53] and those reported in Ref. 11 for MIL-125-NH_2. For a complementary review on MOF-based catalysts for this reaction, please refer to the work of Aguirre-Díaz et al.[49]

The experiments conducted in the absence of MIL-125-NH_2 show that the reaction can proceed also without the MOF with a yield of 40% and that this result is almost unaffected by the irradiation conditions used. This means that the benzylamine coupling happens just because of the heating. If the MOF is added to the reaction, the yield significantly increases up to 78% only if the irradiating light includes the $385 < \lambda < 450$ nm range. This result confirms the photocatalytic activity of the MOF and in particular the role of the amino group in determining its activity. The UV-Vis spectrum of the unfunctionalized MIL-125 is reported as black line in Figure 2b. The titanium oxides nanoclusters in the material absorb the light in the region below 350 nm. The coincidence of the yield obtained by exploiting the full spectral range of the lamp and that using only $\lambda > 385$ nm, suggests that the amino group does not play a role only in stabilizing the generated electron-hole couple but also the accessing to its HOMO-LUMO levels allows a larger fraction of electron-

hole couples to be formed. The data reported in Table 1 indicate also that the nanoconfinement of the reagents in the MOF pores does not influence the reaction: the yield in dark conditions for the MOF coincides to that for the blank. This can be explained based on the acetonitrile measurements (see Section 3.1.1.).

Table 1. Yield for the benzylamine condensation reaction in acetonitrile in contact for 6 h over MIL-125-NH_2 in the dark at 60°C and irradiating the batch with a 150 W Xe lamp without and with two different filters, λ >385 nm and λ >450 nm. The yields obtained in absence of the catalyst are also reported for comparison. A small review on the results reported in the literature for MIL-125-NH_2 and other MOFs is also presented.

sample	**irradiating conditions**	**solvent**	**Conversion (%)**
MIL-125-NH_2	without cut-off filters	CH_3CN	78
			>99[a]
	without cut-off filters	DMF	67[a]
	λ >385	CH_3CN	76
	λ >450 nm	CH_3CN	42
	420 < λ < 800 nm	CH_3CN	73[a]
	dark, 60°C	CH_3CN	38
	dark, RT	CH_3CN	0[a]
blank	without cut-off filters	CH_3CN	40
	λ >385	CH_3CN	38
	λ >450 nm	CH_3CN	37
	420 < λ < 800 nm	CH_3CN	0[a]

	dark, 60°C	CH_3CN	38
UiO-67-Et_2L_6	without cut-off filters	CH_3CN	83[b]
Et_2L_6	without cut-off filters	CH_3CN	96[b]
$Mn(ADBEB)_2(DMF)_2$	420 < λ < 800 nm	DMF/DMA	99[c]
Zn-PDI	λ > 420 nm	CH_3CN	74[d]
Zn-PDI	in dark	CH_3CN	3[d]
PCN-222	λ > 420 nm	CH_3CN	100[e]
PCN-222	dark	CH_3CN	0[e]
UNLPF-12	without cut-off filters	CH_3CN	>99[f]
UNLPF-12	dark	CH_3CN	~0[f]
RPF-30-Er	without cut-off filters	CH_3CN	76[g]

[a]After 12 h, 300 W Xe lamp, no heating, 0.1 mmol benzylamine, 5 mg MOF, 2 ml solvent, air, from Ref. 11. [b]Et_2L_6 = $[Ru^{II}(bpy)_2(dcbpy)]Cl_2$ (bpy = 2,2′-bipyridine; dcbpy = 2,2′-bipyridine-5,5′-dicarboxylic acid). After 1 h, 1 mol % catalyst loadings, 5 cm in front of a 300 W Xe lamp and 60°C, air, from Refs. [22, 48]. [c]ADBEB= 4,4′-(diethynylanthracene-9,10-diyl)dibenzoic acid. After 50 min, 0.2 mmol amine, 6 mg MOF, O_2 atmosphere, 300 W xenon arc lamp, 1 mL DMF/DMA (1/1), Ref. [50]. [d]PDI = perylene diimide. After 4 h, amines 1 mmol, Zn-PDI 0.01 mmol (1 mol%) and acetonitrile 5 mL, air, 500W Xe lamp placed in a distance of 25 cm, Ref. [51]. [e]PCN-22 = $Zr_6(\mu_3\text{-}OH)_8(OH)_8(TCPP)_2$ (TCPP = tetrakis(4-carboxyphenyl)porphyrin). After 1 h, 0.1 mmol benzylamine, 5 mg PCN-222, 100 mW cm2 Xe lamp, 3 mL CH3CN, air. Ref. [52]. [f]UNLPF-12 = $SnL[In(COO)_4]_2(BF_4)_2$, H_2L = tetrakis 3,5-bis((4-hydroxycarbonyl)-phenyl)phenylporphine. After 1h, (1.0 µmol, 0.4 mol % catalyst based on porphyrin moiety), benzylamine (0.27 mmol), 1 mL dry CH_3CN, 14 W CFL (distance ≈8 cm), air, Ref. [53]. [g]RPF-30-Er = $[Er_3(Hsfdc)_3(sfdc)_3(H_2O)]\cdot xH_2O$ (H_2sfdc = 9,9′-spirobi[9H-fluorene]-2,2′-dicarboxylic acid). After 18 h, benzylamine (0.05 mmol); catalyst (10 mol %); ACN as the solvent (1 mL); an oxygen atmosphere purged with balloon at 25 °C; 3000K LED 14 W (100 W) of warm light (distance ≈ 8 cm). air, Ref. [49].

3.2.2. Ex situ ATR-FTIR. We monitored in time the reaction photocatalyzed by MIL-125-NH_2 by recording *ex situ* ATR-IR spectra, with the aim to identify key reaction intermediates and to provide some indications about the mechanism followed in our reaction conditions among all those possible. The spectra recorded after 0 and 15 h of irradiation with a solar lamp are reported in

Figure 4a as orange and blue curves, respectively. The spectra were also collected at intermediate reaction times of 1, 3, 5, 6.5, 8.5, and 10 h. These spectra are showed as grey curves in the same figure. We selected the band at 1643 cm^{-1} band associated to the C=N stretching in *N*-benzylidenebenzylamine as the signal to follow the reaction proceeding in time (see Section S2 for the details on this choice). The dependence of the intensity of this band on the reaction time is reported in Figure 4b. The smaller conversion after 6 h reported in Figure 4b than that obtained in the catalytic tests (<30% vs. 73%, respectively) is due to the absence of acetonitrile, which presence has been reported to cause an increase of the reaction rate.[11] It is noteworthy that the MOF spectrum did not show any modification after 15 h even in this very basic environment, and especially changes connected with degradation processes (e.g. change in the carboxylate bands). We verified by IR spectroscopy that the reaction can be stopped at any time by switching off the lamp and storing the reaction batch in the dark at room temperature for long time (15 h). This was verified by comparing the spectra before and after the dark period. For what concerns other bands in the spectra, we observe a continuous decrease in time of the intensity of the signals associated to benzylamine and the parallel increase of the bands associated to *N*-benzylidenebenzylamine (see Figure 4b). Two extra signals than those associated to the reagent and the product can be detected by comparing the reference spectra with the spectrum recorded after 15 h of reaction (see Figures S6 and S7). In particular, it is observed a signal at about 1670 cm^{-1} and a significantly larger intensity of the broad band in the 3200-2000 cm^{-1} range than that in the reference spectra. These two signals grow continuously while the reaction proceeds and they cannot be associated to an increase in the water absorbed by the mixture from the atmosphere. The signal at 3200-2000 cm^{-1} can be associate to a larger presence of generic species able to develop a H-bond. The signal at 1670 cm^{-1} is associated to a carbonyl group, supporting the mechanism suggested by Sun et al.[11]

This band is close to the position of the C=O group in benzaldehyde (1695 cm^{-1}), although it is more likely associated to a C=O species directly linked to an amine group in aromatic compound (having absorption in the range 1680-1630 cm^{-1}), that is to carbinolamine. Preliminary ATR-IR results would agree that the reaction cannot proceed if anhydrous conditions are adopted. Also this result supports indirectly the mechanism in Scheme 1: in fact it is well known that step (a) (and step d, see Section 3.2.3) requires the presence of water to proceed.[3]

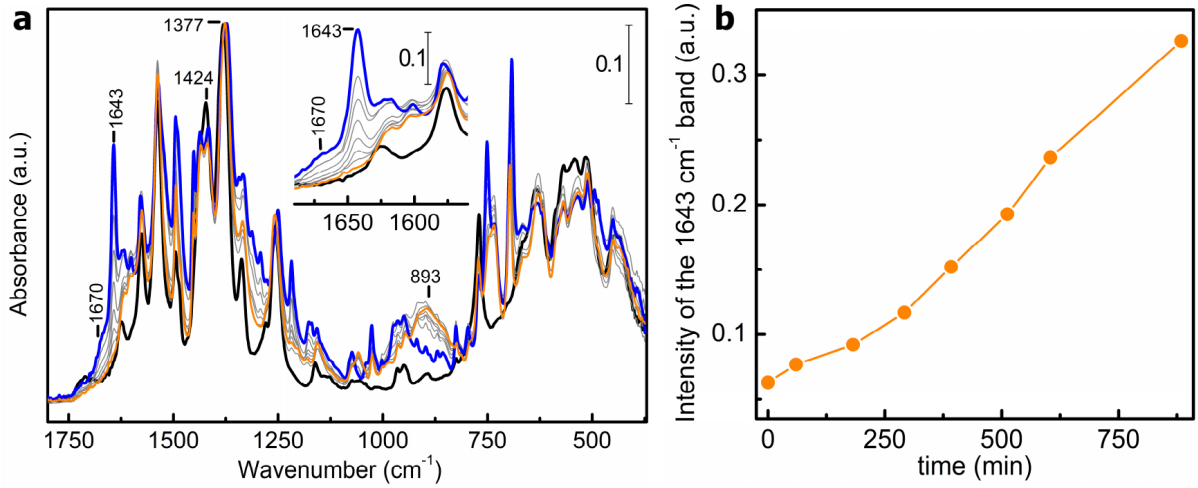

Figure 4. Time evolution of the benzylamine to *N*-benzylideneamine reaction. **a.** *Ex situ* ATR-FTIR spectra of MIL-125-NH_2 solvated with benzylamine recorded after reaction time of 0 (orange line) and 15 h (blue line) at RT in air and upon irradiation in a solar box. Grey lines refer to intermediate time of reaction (1, 3, 5, 6.5, 8.5, and 10 h). Black line refers to the spectrum of the MOF in air. All the spectra have been normalized with respect to the band at 1377 cm^{-1}. In the inset the region around the 1643 cm^{-1} band of *N*-benzylideneamine is shown. **b.** Intensity of the band at 1643 cm^{-1} in the spectra of part **a** as function of the reaction time.

3.2.3. Cluster calculations. The Gibbs free energies calculated for the intramolecular proton transfer in carbinolamine using KS-DFT methods are reported in Figures S8 and S10. The MOF has not been included in the calculations. We have adopted this approximation based on the catalytic tests indicating that the presence of the MOF itself does not influence the reaction in the dark. The A and B conformers of carbinolamine are indicated by the calculations to be almost isoenergetics and their reaction path are equivalent (see Table S5 and Section S.8 in Appendix A). In the following we will discuss only the data obtained for one of them, the conformer A.

The reaction profiles obtained for the A conformer are reported in Figure 2c, considering the proton transfer mediated by zero (black line), one (light blue line), and two water molecules (purple line). It is evident that the presence of water molecules significantly decreases the barrier associated to the proton transfer, from 206 kJ mol^{-1} in anhydrous conditions to 112 and 88 kJ mol^{-1} for one and two H_2O, respectively. The decrease of the ΔG_{TS} on increasing the number of water molecules from zero to two is coincident to that reported for the reaction between methylamine and formaldehyde[38] (~120 kJ mol^{-1}). The calculations would suggest that the presence of water is necessary for the reaction to proceed not only in the step (a), notoriously water mediated, but also for step (d).

A structural change is also observed in the TS upon increasing the hydration degree. In particular the C-O bond length increases from 1.855 for the zero molecules case to 2.398 and 2.337 Å for the 1 and 2 H_2O molecules, respectively (for the 2 H_2O molecules cluster, see Figure 2d, green dotted line). A slight increase is also observed in **CA** (from 1.412 Å to 1.433 and 1.436 Å, for 0, 1, and 0 H_2O molecules respectively), that can be explained as the carbinolamine being more prone to dehydrate in presence of molecules that can mediate the proton transfer. The N-H bond does not

change significantly in **CA** upon hydration. The increased number of water molecules also decreases the planarity of the **TS**.

For what concerns the solvent, it has been proven experimentally that a polar solvent can increase the conversion in imine formation.[3, 11] This is likely associated to the polar nature of the TS that can be then stabilized by the presence of the solvent. An important role of the solvent as a proton shuttle has been excluded based on previous experiments on imine formation.[3, 11] Accordingly, the calculations indicate a decrease of the barrier by inclusion of the reaction medium as implicit solvent with respect to the gas phase case, although its effect is lower than that of the water.

4. CONCLUSIONS

MIL-125-NH_2(Ti) was synthesized and tested as photocatalyst for the aerobic benzylamine condensation to *N*-benzylidenebenzylamine, determining a yield of 78% in acetonitrile after irradiating the batch with a Xe lamp for 6 h. Using different irradiating conditions, we verified the photocatalytic activity of MIL-125-NH_2 and the important role of the amino group in determining the MOF photo-activity under visible light. The band gap of MOFs based on closed-shell metal ions is mainly determined by the electronic levels of the organic linkers.[54] Among common functional groups, the amino group is the functionality determining the smallest band gap. Moreover, the band gap narrows on increasing the number of amino functional groups.[54] We can then conclude that the efficiency of the catalyst can be improved increasing the number of amino groups on the linker, in analogy to what has been reported for other reactions,[28, 55]

The comparison between the results obtained in the dark and in absence of the catalyst proved the negligible influence of the MOF surface on the reaction. This result is in agreement with the absence of strong polarizing centres on its surface as indicated by acetonitrile measurements. The reaction has been followed in time using *ex situ* infrared spectroscopy. The presence of a signal at 1670 cm^{-1} would support the mechanism suggested previously by Sun et al.[11] that considers the oxidation of one benzylamine molecule to benzaldehyde as first step of the reaction. Cluster calculations on the last step of the reaction (i.e., the intramolecular proton transfer in carbinolamine) strongly suggests that, although water is not recommended as solvent in this reaction because it is often associated to low selectivity, the presence of water impurities can facilitate the reaction to proceed at temperature close to RT. The preferential adsorption of water molecules upon acetonitrile in the MOF pores can be facilitated for example by increasing the number of amino groups on the linker, that is by increasing the hydrophilicity of the MOF.[56] Nevertheless, the energetic barrier associated to this step is computed to be 88 kJ mol^{-1} that is it has still room for improvements. Strategies aimed to decrease the energy of its **TS** should be foreseen to improve the kinetics. Two possible directions can be suggested on the basis of the results obtained in this work. We verified that MIL-125-NH_2(Ti) surface is not able to influence the reaction. One possibility to allow the involvement of the MOF in the reaction beyond the O_2 oxidation step, can be the introduction of charged species in the MIL-125-NH_2 pores in order to facilitate the adsorption of the reagents on the MOF surface and then their coupling reaction. Another possibility would be to decrease the pH of the reaction mixture. The mechanism reported in Scheme 1 is known to work in neutral and basic conditions. In acid conditions, although amine protonation can likely happen, so avoiding the reaction to proceed, the last step is substituted by

the iminium ion formation that is known to ask for lower energetic barrier in the intramolecular proton transfer that that required for the formation of the neutral imine.

ASSOCIATED CONTENT

Supporting Information.

The following files are available free of charge.

Additional experimental details, textural properties, additional IR spectra of reference compounds and concerning the reaction, additional data on the computed mechanism for CA to BI conversion, XYZ coordinates of all optimized periodic and cluster models (file type, PDF)

AUTHOR INFORMATION

Corresponding Author

*Department of Science and High Technology and INSTM, University of Insubria, Via Valleggio 9, 22100 Como, Italy. Phone: +39 031 238 6623. E-mail address: jg.vitillo@gmail.com

Present Addresses

†RTI International, Research Triangle Park, NC 27709-2194, USA.

Author Contributions

The manuscript was written through contributions of all authors.

Funding Sources

Spanish Government through projects MAT2017-82288-C2-1-P and the Severo Ochoa program (SEV-2016-0683).

ABBREVIATIONS

MOFs = Metal organic frameworks, FTIR = Fourier transformed infrared, LCCT = ligand-to-cluster charge transfer, KS-DFT = Kohn-Sham Density Functional Theory, TS = transition state.

ACKNOWLEDGMENT

Bartolomeo Civalleri is acknowledged for the kind help with the calculations. Financial support by the Spanish Government is acknowledged through projects MAT2017-82288-C2-1-P and the Severo Ochoa program (SEV-2016-0683).

REFERENCES

1. Opris, C. M.; Pavel, O. D.; Moragues, A.; El Haskourib, J.; Beltran, D.; Amoros, P.; Marcos, M. D.; Stoflea, L. E.; Parvulescu, V. I., New multicomponent catalysts for the selective aerobic oxidative condensation of benzylamine to N-benzylidenebenzylamine. *Catal. Sci. Tech.* **2014,** 4, 4340-4355.
2. Belowich, M. E.; Stoddart, J. F., Dynamic imine chemistry. *Chem. Soc. Rev.* **2012,** 41, 2003-2024.
3. Ciaccia, M.; Di Stefano, S., Mechanisms of imine exchange reactions in organic solvents. *Org. Biomol. Chem.* **2015,** 13, 646-654 and references therein.
4. Mukaiyama, T.; Kawana, A.; Fukuda, Y.; Matsuo, J.-i., Oxidation of Various Secondary Amines to Imines with N-tert-Butylphenylsulfinimidoyl Chloride. *Chem. Lett.* **2001,** 30, 390-391.
5. Deb, M.; Hazra, S.; Dolui, P.; Elias, A. J., Ferrocenium Promoted Oxidation of Benzyl Amines to Imines Using Water as the Solvent and Air as the Oxidant. *ACS Sustainable Chem. Eng.* **2019,** 7, 479-486.
6. Largeron, M.; Fleury, M.-B., Bioinspired Oxidation Catalysts. *Science* **2013,** 339, 43.
7. Su, C.; Acik, M.; Takai, K.; Lu, J.; Hao, S.-j.; Zheng, Y.; Wu, P.; Bao, Q.; Enoki, T.; Chabal, Y. J., et al., Probing the catalytic activity of porous graphene oxide and the origin of this behaviour. *Nature Commun.* **2012,** 3, 1298.
8. Samec, J. S. M.; Éll, A. H.; Bäckvall, J.-E., Efficient Ruthenium-Catalyzed Aerobic Oxidation of Amines by Using a Biomimetic Coupled Catalytic System. *Chem. Eur. J.* **2005,** 11, 2327-2334.
9. Murahashi, S.-I., Synthetic Aspects of Metal-Catalyzed Oxidations of Amines and Related Reactions. *Angew. Chem. Int. Ed.* **1995,** 34, 2443-2465.

10. Liu, H.; Xu, C.; Li, D.; Jiang, H.-L., Photocatalytic Hydrogen Production Coupled with Selective Benzylamine Oxidation over MOF Composites. *Angew. Chem. Int. Ed.* **2018,** 57, 5379-5383.
11. Sun, D.; Ye, L.; Li, Z., Visible-light-assisted aerobic photocatalytic oxidation of amines to imines over NH_2-MIL-125(Ti). *Appl. Catal. B* **2015,** 164, 428-432.
12. Chen, B.; Wang, L.; Gao, S., Recent Advances in Aerobic Oxidation of Alcohols and Amines to Imines. *ACS Catal.* **2015,** 5, 5851-5876.
13. Li, S.; Li, G.; Ji, P.; Zhang, J.; Liu, S.; Zhang, J.; Chen, X., A Giant Mo/Ta/W Ternary Mixed-Addenda Polyoxometalate with Efficient Photocatalytic Activity for Primary Amine Coupling. *ACS Appl. Mater. Interfaces* **2019,** 11, 43287-43293.
14. Furukawa, H.; Cordova, K. E.; O'Keeffe, M.; Yaghi, O. M., The Chemistry and Applications of Metal-Organic Frameworks. *Science* **2013,** 341.
15. Rogge, S. M. J.; Bavykina, A.; Hajek, J.; Garcia, H.; Olivos-Suarez, A. I.; Sepúlveda-Escribano, A.; Vimont, A.; Clet, G.; Bazin, P.; Kapteijn, F., et al., Metal–organic and covalent organic frameworks as single-site catalysts. *Chem. Soc. Rev.* **2017,** 46, 3134-3184.
16. Corma, A.; García, H.; Llabrés i Xamena, F. X., Engineering Metal Organic Frameworks for Heterogeneous Catalysis. *Chem. Rev.* **2010,** 110, 4606-4655.
17. Llabres i Xamena, F.; Gascon, J., *Metal Organic Frameworks as Heterogeneous Catalysts*. The Royal Society of Chemistry: Cambridge, 2013.
18. Vitillo, J. G.; Crocellà, V.; Bonino, F., ZIF-8 as a Catalyst in Ethylene Oxide and Propylene Oxide Reaction with CO_2 to Cyclic Organic Carbonates. *ChemEngineering* **2019,** 3, 60.
19. Beyzavi, M. H.; Vermeulen, N. A.; Howarth, A. J.; Tussupbayev, S.; League, A. B.; Schweitzer, N. M.; Gallagher, J. R.; Platero-Prats, A. E.; Hafezi, N.; Sarjeant, A. A., et al., A Hafnium-Based Metal–Organic Framework as a Nature-Inspired Tandem Reaction Catalyst. *J. Amer. Chem. Soc.* **2015,** 137, 13624-13631.
20. Yang, D.; Gates, B. C., Catalysis by Metal Organic Frameworks: Perspective and Suggestions for Future Research. *ACS Catal.* **2019,** 9, 1779-1798.
21. Dhakshinamoorthy, A.; Alvaro, M.; Garcia, H., Aerobic Oxidation of Benzyl Amines to Benzyl Imines Catalyzed by Metal–Organic Framework Solids. *Chem. Cat. Chem.* **2010,** 2, 1438-1443.
22. Wang, J.-L.; Wang, C.; Lin, W., Metal–Organic Frameworks for Light Harvesting and Photocatalysis. *ACS Catal.* **2012,** 2, 2630-2640.
23. Kampouri, S.; Stylianou, K. C., Dual-Functional Photocatalysis for Simultaneous Hydrogen Production and Oxidation of Organic Substances. *ACS Catal.* **2019,** 9, 4247-4270.
24. Zhu, J.; Li, P.-Z.; Guo, W.; Zhao, Y.; Zou, R., Titanium-based metal–organic frameworks for photocatalytic applications. *Coord. Chem. Rev.* **2018,** 359, 80-101.
25. Fu, Y.; Sun, L.; Yang, H.; Xu, L.; Zhang, F.; Zhu, W., Visible-light-induced aerobic photocatalytic oxidation of aromatic alcohols to aldehydes over Ni-doped NH_2-MIL-125(Ti). *Appl. Catal. B* **2016,** 187, 212-217.
26. Kampouri, S.; Nguyen, T. N.; Ireland, C. P.; Valizadeh, B.; Ebrahim, F. M.; Capano, G.; Ongari, D.; Mace, A.; Guijarro, N.; Sivula, K., et al., Photocatalytic hydrogen generation from a visible-light responsive metal–organic framework system: the impact of nickel phosphide nanoparticles. *J. Mater. Chem. A* **2018,** 6, 2476-2481.
27. Cadiau, A.; Kolobov, N.; Srinivasan, S.; Goesten, M.; Haspel, H.; Bavykina, A.; Tchalala, M.; Maity, P.; Goryachev, A.; Poryvaev, A., et al., A new Titanium Metal Organic Framework

with visible-light responsive photocatalytic activity. *Angew. Chem. Int. Ed.* **2020**, https://doi.org/10.1002/anie.202000158.
28. Hendon, C. H.; Tiana, D.; Fontecave, M.; Sanchez, C.; D'arras, L.; Sassoye, C.; Rozes, L.; Mellot-Draznieks, C.; Walsh, A., Engineering the Optical Response of the Titanium-MIL-125 Metal–Organic Framework through Ligand Functionalization. *J. Amer. Chem. Soc.* **2013,** 135, 10942-10945.
29. Guo, H.; Lin, F.; Chen, J.; Li, F.; Weng, W., Metal–organic framework MIL-125(Ti) for efficient adsorptive removal of Rhodamine B from aqueous solution. *Appl. Organomet. Chem.* **2015,** 29, 12-19.
30. Kim, S.-N.; Kim, J.; Kim, H.-Y.; Cho, H.-Y.; Ahn, W.-S., Adsorption/catalytic properties of MIL-125 and NH2-MIL-125. *Catal. Today* **2013,** 204, 85-93.
31. Dan-Hardi, M.; Serre, C.; Frot, T.; Rozes, L.; Maurin, G.; Sanchez, C.; Férey, G., A New Photoactive Crystalline Highly Porous Titanium(IV) Dicarboxylate. *J. Amer. Chem. Soc.* **2009,** 131, 10857-10859.
32. Dhakshinamoorthy, A.; Asiri, A. M.; García, H., Metal–Organic Framework (MOF) Compounds: Photocatalysts for Redox Reactions and Solar Fuel Production. *Angew. Chem. Int. Ed.* **2016,** 55, 5414-5445.
33. Fu, Y.; Yang, H.; Du, R.; Tu, G.; Xu, C.; Zhang, F.; Fan, M.; Zhu, W., Enhanced photocatalytic CO_2 reduction over Co-doped NH_2-MIL-125(Ti) under visible light. *RSC Adv.* **2017,** 7, 42819-42825.
34. Tan, X.; Zhang, J.; Shi, J.; Cheng, X.; Tan, D.; Zhang, B.; Liu, L.; Zhang, F.; Han, B.; Zheng, L., Fabrication of NH_2-MIL-125 nanocrystals for high performance photocatalytic oxidation. *Sustainable Energy Fuels* **2020,** 4, 2823-2830.
35. Santaclara, J. G.; Nasalevich, M. A.; Castellanos, S.; Evers, W. H.; Spoor, F. C. M.; Rock, K.; Siebbeles, L. D. A.; Kapteijn, F.; Grozema, F.; Houtepen, A., et al., Organic Linker Defines the Excited-State Decay of Photocatalytic MIL-125(Ti)-Type Materials. *Chem. Sus. Chem.* **2016,** 9, 388-395.
36. Nasalevich, M. A.; Hendon, C. H.; Santaclara, J. G.; Svane, K.; van der Linden, B.; Veber, S. L.; Fedin, M. V.; Houtepen, A. J.; van der Veen, M. A.; Kapteijn, F., et al., Electronic origins of photocatalytic activity in d^0 metal organic frameworks. *Sci. Rep.* **2016,** 6, 23676.
37. Alvaro, M.; Carbonell, E.; Ferrer, B.; Llabrés i Xamena, F. X.; Garcia, H., Semiconductor Behavior of a Metal-Organic Framework (MOF). *Chem. Eur. J.* **2007,** 13, 5106-5112.
38. Hall, N. E.; Smith, B. J., High-Level ab Initio Molecular Orbital Calculations of Imine Formation. *J. Phys. Chem. A* **1998,** 102, 4930-4938.
39. Jiménez, M. V.; Fernández-Tornos, J.; González-Lainez, M.; Sánchez-Page, B.; Modrego, F. J.; Oro, L. A.; Pérez-Torrente, J. J., Mechanistic studies on the N-alkylation of amines with alcohols catalysed by iridium(i) complexes with functionalised N-heterocyclic carbene ligands. *Catal. Sci. Technol.* **2018,** 8, 2381-2393.
40. Vitillo, J. G.; Bordiga, S., Increasing the stability of Mg_2(dobpdc) metal-organic framework in air through solvent removal. *Mater. Chem. Front.* **2017,** 1, 444-448.
41. Gregg, S. J.; Sing, K. S. W., *Adsorption, surface area and porosity (2nd ed.)*. Academic Press Inc.: London, 1982.
42. Bonino, F.; Lamberti, C.; Chavan, S.; Vitillo, J. G.; Bordiga, S., Characterization of MOFs. 1. Combined Vibrational and Electronic Spectroscopies. In *Metal Organic Frameworks as Heterogeneous Catalysts*, Llabrés i Xamena, F., Gascon, J., Eds. RSC Catalysis Series: Cambridge, 2013; pp 76-142.

43. Fu, Y.; Sun, D.; Chen, Y.; Huang, R.; Ding, Z.; Fu, X.; Li, Z., An Amine-Functionalized Titanium Metal–Organic Framework Photocatalyst with Visible-Light-Induced Activity for CO2 Reduction. *Angew. Chem. Int. Ed.* **2012,** 51, 3364-3367.
44. Morterra, C.; Peñarroya Mentruit, M.; Cerrato, G., Acetonitrile adsorption as an IR spectroscopic probe for surface acidity/basicity of pure and modified zirconias. *Phys. Chem. Chem. Phys.* **2002,** 4, 676-687.
45. Pazé, C.; Bordiga, S.; Lamberti, C.; Salvalaggio, M.; Zecchina, A.; Bellussi, G., Acidic Properties of H^+ Zeolite As Probed by Bases with Proton Affinity in the 118-204 kcal mol^{-1} Range: A FTIR Investigation. *J. Phys. Chem. B* **1997,** 101, 4740-4751.
46. Bonino, F.; Damin, A.; Bordiga, S.; Lamberti, C.; Zecchina, A., Interaction of CD_3CN and Pyridine with the Ti(IV) Centers of TS-1 Catalysts: a Spectroscopic and Computational Study. *Langmuir* **2003,** 19, 2155-2161.
47. Escalona Platero, E.; Peñarroya Mentruit, M.; Morterra, C., Fourier Transform Infrared Spectroscopy Study of CD3CN Adsorbed on Pure and Doped γ-Alumina. *Langmuir* **1999,** 15, 5079-5087.
48. Wang, C.; Xie, Z.; deKrafft, K. E.; Lin, W., Doping Metal–Organic Frameworks for Water Oxidation, Carbon Dioxide Reduction, and Organic Photocatalysis. *J. Am. Chem. Soc.* **2011,** 133, 13445-13454.
49. Aguirre-Díaz, L. M.; Snejko, N.; Iglesias, M.; Sánchez, F.; Gutiérrez-Puebla, E.; Monge, M. Á., Efficient Rare-Earth-Based Coordination Polymers as Green Photocatalysts for the Synthesis of Imines at Room Temperature. *Inorg. Chem.* **2018,** 57, 6883-6892.
50. Liu, H.; Guo, Z.; Lv, H.; Liu, X.; Che, Y.; Mei, Y.; Bai, R.; Chi, Y.; Xing, H., Visible-light-driven self-coupling and oxidative dehydrogenation of amines to imines via a Mn(II)-based coordination polymer. *Inorg. Chem. Front.* **2020,** 7, 1016-1025.
51. Zeng, L.; Liu, T.; He, C.; Shi, D.; Zhang, F.; Duan, C., Organized Aggregation Makes Insoluble Perylene Diimide Efficient for the Reduction of Aryl Halides via Consecutive Visible Light-Induced Electron-Transfer Processes. *J. Amer. Chem. Soc.* **2016,** 138, 3958-3961.
52. Xu, C.; Liu, H.; Li, D.; Su, J.-H.; Jiang, H.-L., Direct evidence of charge separation in a metal–organic framework: efficient and selective photocatalytic oxidative coupling of amines via charge and energy transfer. *Chem. Sci.* **2018,** 9, 3152-3158.
53. Johnson, J. A.; Luo, J.; Zhang, X.; Chen, Y.-S.; Morton, M. D.; Echeverría, E.; Torres, F. E.; Zhang, J., Porphyrin-Metalation-Mediated Tuning of Photoredox Catalytic Properties in Metal–Organic Frameworks. *ACS Catal.* **2015,** 5, 5283-5291.
54. Ryder, M. R.; Donà, L.; Vitillo, J. G.; Civalleri, B., Understanding and Controlling the Dielectric Response of Metal–Organic Frameworks. *ChemPlusChem* **2018,** 83, 308-316.
55. Chambers, M. B.; Wang, X.; Ellezam, L.; Ersen, O.; Fontecave, M.; Sanchez, C.; Rozes, L.; Mellot-Draznieks, C., Maximizing the Photocatalytic Activity of Metal–Organic Frameworks with Aminated-Functionalized Linkers: Substoichiometric Effects in MIL-125-NH_2. *J. Am. Chem. Soc.* **2017,** 139, 8222-8228.
56. Caratelli, C.; Hajek, J.; Cirujano, F. G.; Waroquier, M.; Llabrés i Xamena, F. X.; Van Speybroeck, V., Nature of active sites on UiO-66 and beneficial influence of water in the catalysis of Fischer esterification. *J. Catal.* **2017,** 352, 401-414.

TOC/Abstract Graphic.